

Tunable Plasmonic Properties and Absorption Enhancement in Terahertz Photoconductive Antenna Based on Optimized Plasmonic Nanostructures

Tatjana Gric^{1,2} · Andrei Gorodetsky^{3,4} ·
Aleksej Trofimov¹ · Edik Rafailov⁵

Received: 6 April 2018 / Accepted: 21 June 2018 / Published online: 28 June 2018
© Springer Science+Business Media, LLC, part of Springer Nature 2018

Abstract Herein, we numerically investigate terahertz photoconductive antennas (PCAs) based on optimized plasmonic nanostructures and absorption enhancement in nanocylinders. Plasmonic behavior in the visible to near-infrared light spectrum is achievable due to the metallic nanostructure employment. Herein, we study the absorption enhancement of silver and transparent-conducting oxides (TCO) nanocylinders with different diameters by means of effective medium approximation. This study also reports on the stronger enhancement in the case of TCO nanocylinders. The results show that resonant absorption amplitude and wavelength are dramatically affected by the thickness of the nanostructure as well as by the distances between nanocylinders. The outputs reported here provide a fertile ground for precise control of the nanowire structures for sensing and other enhanced optical applications. It is worthwhile noting that in case of TCO nanocylinders, absorption enhancement for NIR wavelengths, being relevant for present terahertz generation setup, reaches up to fivefold leading to 25-fold increase in terahertz radiation.

Keywords Absorption · Terahertz photoconductive antenna · Nanostructure · Metamaterial

✉ Tatjana Gric
tatjana.gric@vgtu.lt

¹ Department of Electronic Systems, Vilnius Gediminas Technical University, Vilnius, Lithuania

² Semiconductor Physics Institute, Center for Physical Sciences and Technology, Vilnius, Lithuania

³ ITMO University, St. Petersburg, Russia 197101

⁴ Department of Chemistry, Imperial College London, London SW7 2AZ, UK

⁵ Aston Institute of Photonic Technologies, Aston University, Birmingham B4 7ET, UK

1 Introduction

In the last decade, the fast-growing interest in (THz) spectrum played an important role allowing for potential applications in security and medical imaging, spectroscopy, and indoor communication [1–7]. Because of compact structure, simple fabrication and room temperature operation [8], photoconductive antennas (PCAs) provide terahertz wave generation and detection. Moreover, PCAs are widely used in time domain terahertz imaging and spectroscopy systems for generating pulsed terahertz radiation [4, 9].

Metallic nanostructures playing an important role in nanophotonic applications are a hot topic nowadays. Such applications are possible due to their capability to focus or intensify electromagnetic fields close to the metal by employing excitation approach of surface plasmon polaritons (SPPs) [10–12]. Plasmonic composites for instance nanoparticle pairs or dimers have been recently proposed for surface-enhanced Raman spectroscopy (SERS) application [13, 14] because of the electromagnetic “hotspots” generated between nanoparticles. Doing so, the Raman enhancement phenomenon takes place enabling the detection of single molecules [15]. Though, pure control of stability of the hotspots associated with nanoparticle collections achieved using ordinary approaches stands for as the significant problem.

A type of extremely reproducible and stable composites is named as “metamaterials.” Moreover, metamaterials can be utilized for the electromagnetic environment with homogeneously located hotspots, opening the wide avenues for SERS-based applications [16, 17] besides their possible applications in negative refractive index materials and perfect lensing [18, 19]. Aiming to obtain effective negative permeability [20], split-ring resonators (SRRs) usually serve as main components for metamaterials. An asymmetric double split ring (ADSR) possesses two splits with a pair of arcs of different lengths on the contrary to the basic SRR with a single split. It should be mentioned that a trapped mode in ADSR might serve as a basis for frequency-selective thin-film sensors [21]. Though, it is impossible to use this mode for SERS applications. Above and beyond, field enhancement and hotspot pattern in ADSR providing a fertile ground for SERS applications have not been studied. In recent years, a lot of research has been done towards application of plasmonic optical nanoantennas for terahertz generation enhancement. It has been concluded that the former approach offers high fs-laser pump absorption, shorter photocarrier lifetimes, and exceptional thermal efficiency [22]. Thus, one may realize terahertz modulation with metamaterials [23]. Moreover, it has been recently reported that it is possible to modulate the transmission of a terahertz pulse through metamaterial [23] and plasmonic structures by means of optical pumping around the resonance frequencies of these structures. Besides the fact that using techniques such as electron beam lithography [24] has provided some advantages, improvements are needed in high-throughput fabrication techniques.

Here, we deal with the concept of hybrid terahertz-optical PCAs similar to [25] by comprehensive numerical optimization of a log-periodic terahertz photoconductive antenna coupled to a silver (Ag) [26] or transparent conducting oxide (TCO) nanoantenna array arranged in the gap of the terahertz antenna. The light is shed on the operation principles of the resulting hybrid terahertz antenna. Doing so, an approach to significantly boost the antenna performance is provided. Tuning the dimensions of nanoantennas and the distance between them allows to achieve an enhancement of optical-to- terahertz conversion efficiency.

2 Basic Concept

The structure of a nanowire composite is outlined in Fig. 1. The nanowire radius is denoted as R . In order to see the effect of absorption enhancement, we have chosen Ag and/or TCO as the nanowire material. Figure 1 shows the phenomenon of the embedded nanoantennas in the semiconductor host which have permittivities ε_n and ε_{GaAs} , respectively. Moreover, the fill ratio of nanocylinders (ρ) in the host material can be defined as follows:

$$\rho = \frac{\text{nanowire area}}{\text{unit cell area}} \quad (1)$$

The dielectric function of the doped GaAs layer is calculated by means of the Drude dielectric function $\varepsilon_{GaAs}(\omega) = \varepsilon_\infty - \omega_p^2 / (\omega^2 + i\omega/\tau)$, where $\varepsilon_\infty = 12.96$, $\omega_p^2 = ne^2 / \varepsilon_0 m_{eff}$ with $m_{eff} = 0.067m_e$, and $\tau = 0.1$ ps is the scattering time. The electron concentration in the GaAs layer is typically $n = 5 \times 10^{18} \text{ cm}^{-3}$ [27]. The dielectric function of the nanocylinders deserves special attention due to the fact that two cases, i.e., silver and TCO nanocylinders, have been considered. A phenomenon of high-conducting metal-doped semiconducting oxides being transparent has given rise to potential applications recently. Due to a metal being opaque for light, the issue is of unprecedented interest for the community. From the application view point, transparent conducting metals characterized by high DC conductivity (σ_{DC}) are anticipated for optoelectronic devices, ranging from solar cells to electronic paper, touch screens, and displays. However, since $\sigma_{DC} = ne^2\tau/m$ of a metal is associated with plasmon frequency $\omega_p^2 = ne^2 / \varepsilon_0 m$ through the free-electron density n_e , a high-conducting metal (with a high n_e) is naturally opaque for light due to its permittivity ε being usually very negative caused by its high ω_p . Typical approaches to fabricate transparent conducting metal-doped semiconducting oxides are to increase the n_e , by means of transparent conducting oxides (TCOs). Table 1 presents the parameters of Drude-Lorentz approach for AZO, GZO, and ITO obtained from experimental data [28].

Aiming to study the light-induced photoconductivity in metal and TCO nanowire-enhanced semiconductor, we need to look into a nanowire as a waveguide for the pump light.

Fig. 1 A schematic view of an anisotropic nanowire composite

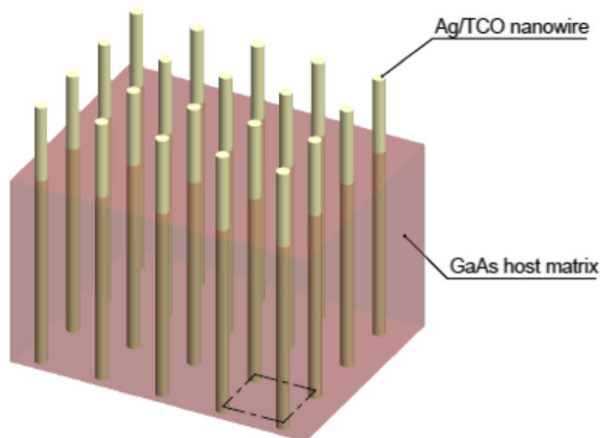


Table 1 Drude-Lorentz parameters of plasmonic materials based on experimental data. One may approximate the material dielectric function by the equation: $\epsilon_{TCO} = \epsilon_b - \frac{\omega_p^2}{\omega(\omega + i\gamma_p)} + \frac{f_1\omega_1^2}{(\omega_1^2 - \omega^2 - i\omega\gamma_1)}$, with the values of the parameters outlined in the table [28]

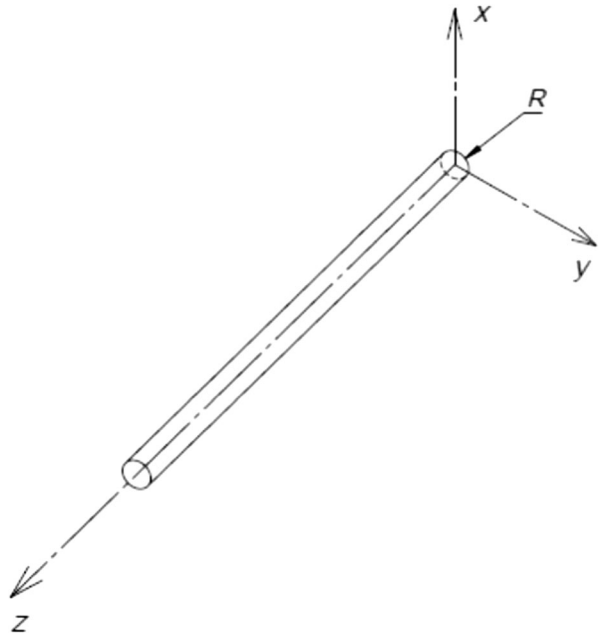
| | AZO | GZO | ITO | TiN (deposited at 800 °C) | TiN (deposited at 500 °C) | ZrN |
|-----------------|---------|--------|--------|---------------------------|---------------------------|--------|
| ϵ_b | 3.5402 | 3.2257 | 3.528 | 4.855 | 2.485 | 3.4656 |
| ω_p [eV] | 1.7473 | 1.9895 | 1.78 | 7.9308 | 5.953 | 8.018 |
| γ_p [eV] | 0.04486 | 0.1229 | 0.155 | 0.1795 | 0.5142 | 0.5192 |
| f_1 | 0.5095 | 0.3859 | 0.3884 | 3.2907 | 2.0376 | 2.4509 |
| ω_1 [eV] | 4.2942 | 4.050 | 4.210 | 4.2196 | 3.9545 | 5.48 |
| γ_1 [eV] | 0.1017 | 0.0924 | 0.0919 | 2.0341 | 2.4852 | 1.7369 |

3 Wave Propagation on Anisotropic Cylindrical Waveguides

The components of ϵ^{eff} may be dramatically influenced by the dispersion as it has been found for gigahertz systems in [29–32]. Aiming to classify the modes propagating in a planar waveguide having a composite core made of a rectangular arrangement of Ag/TCO nanocylinders in GaAs host and to clarify these effects, we used MATLAB package. Waves propagate in a cylindrical waveguide. The axis of the waveguide is along z -direction as displayed in Fig. 2. The waveguide is nonmagnetic and possesses an anisotropic optical feature

$$\epsilon_x = \epsilon_y = \epsilon_t \neq \epsilon_z \tag{2}$$

Fig. 2 A view of an anisotropic cylindrical waveguide



A waveguide with a radius a will be studied making an assumption for the permittivity as follows:

$$\epsilon_t = \rho\epsilon_n + (1-\rho)\epsilon_{GaAs} \tag{3}$$

$$\epsilon_z = \frac{(1 + \rho)\epsilon_n\epsilon_{GaAs} + (1-\rho)\epsilon_{GaAs}^2}{(1 + \rho)\epsilon_{GaAs} + (1-\rho)\epsilon_n} \tag{4}$$

It is worthwhile noting that the propagation of TE and TM modes in a waveguide with anisotropic core is defined as follows

$$\frac{\pi^2}{\epsilon_y d^2} + \frac{k^{(TE)^2}}{\epsilon_y} = \frac{\omega^2}{c^2}, \quad \frac{\pi^2}{\epsilon_x d^2} + \frac{k^{(TM)^2}}{\epsilon_z} = \frac{\omega^2}{c^2} \tag{5}$$

where k , c , and d are being the wave vector, speed of light in the vacuum, and the waveguide thickness, correspondingly [33]. One may calculate $\text{Im}(k^{(TE)})$ aiming to evaluate the absorption.

One may define the total scattering cross-section (SCS) as a ratio of the total scattered power to the intensity of the incident plane wave. Doing so, it can be calculated as [34]:

$$SCS = \frac{2\lambda}{\pi\sqrt{\epsilon_n + 1}} \sum_{m=-\infty}^{+\infty} |\rho_m|^2 \tag{6}$$

where ρ_m are the m th mode expansion coefficients [34]. We will follow [35] and introduce normalized scattering cross-section (NSCS) by normalizing all SCS values to $2\lambda\pi$.

4 Results and Discussion

The terahertz photoconductive switches or PCAs [36] stand for as the most widely used source of coherent pulsed terahertz radiation. Figure 3 displays a typical realization of such terahertz antenna in log-periodic design. At this point, two conductive electrodes separated by a gap are placed onto a semiconductor. Optical nanoantennas are resonant nanostructures being able to transform incident optical waves into a strongly localized near-field [26, 37]. One may call the nanoantenna-based PCAs as hybrid terahertz-optical PCAs. The schematic presentation of such antenna is illustrated in Fig. 3. Here, the minor radius of the nanocylinder has been fixed

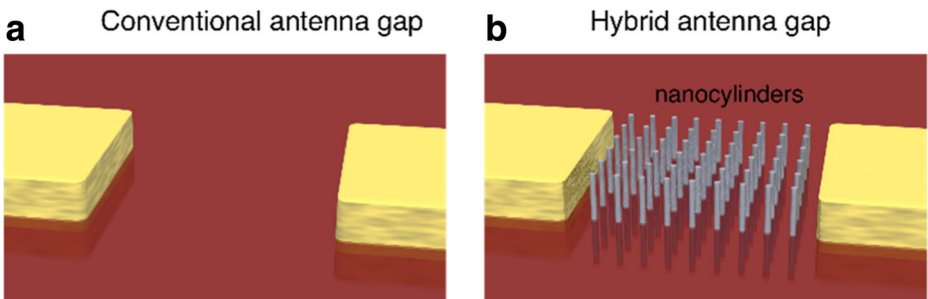


Fig. 3 Conventional (a) and silver nanoantenna-loaded hybrid (b) photoconductive terahertz antenna

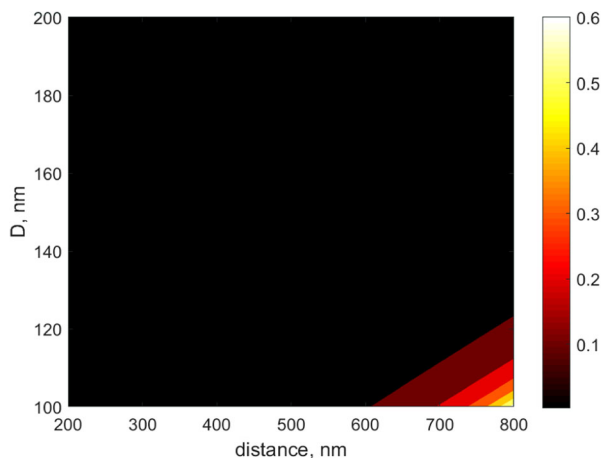
to 50 nm. Such nanocylinders are typical for our fabrication facilities [38]. One may calculate the absorption enhancement as the power absorbed in GaAs surface film with silver nanoantenna array normalized to the power absorbed in the GaAs film without nanoantennas.

Figures 4 and 5 display the calculated absorption enhancement at the wavelength of 800 nm as a dependence of the nanoantenna radius R and distance between nanoantenna centers. The absorption enhancement has been calculated as the absorption in the nanostructure-enhanced structure normalized by the absorption in plain GaAs substrate.

Figure 4 presents absorption enhancement calculated for our design with silver defined by a Drude approach $\varepsilon_{Ag}(\omega) = 5 - \omega_p^2 / (\omega(\omega + i\Gamma))$ with $\omega_p = 1.37 \times 10^{16}$ hertz and $\Gamma = 2.73 \times 10^{13}$ hertz according to [39]. Moreover, the examples of the stronger enhancement are demonstrated for the TCO nanocylinder case in Fig. 5. Thus, in Fig. 5(d–f), it is clearly seen that there are strong local maxima of the absorption enhancement in the simulation map accompanied by few “hot spots” in the map. For instance, the maximum in case of TiN (deposited at 800 °C) nanocylinders is in the range of the diameter 140–200 nm and in range of distances 200–300 nm. The absorption maximum in case of TiN (deposited at 500 °C) is at the distances of 200–250 nm for the particles with diameter ranging between 160 and 200 nm. Thus, from these numerical calculations, we may expect significant enhancement of the terahertz PCA performance with such optimized plasmonic nanostructures. Fivefold pump absorption enhancement can potentially lead to 25-fold increase in terahertz spectral intensity enhancement [40]; however, due to high conductivity of silver, and to a far lesser degree in oxides, overall PCA dark resistance could rise, thus leading to lower yet reasonable terahertz conversion efficiency enhancement [22]. Tailoring the size of silver nanoantennas and their arrangement allows for an obtained experimental enhancement of optical-to- terahertz conversion efficiency [38]. Moreover, a cost-effective fabrication technique to realize such hybrid terahertz antennas with optimized plasmonic nanostructures via thermal dewetting process has been proposed. Doing so, no post-processing is required ending up with the proposed solution being very attractive for applications.

We have also calculated absorption enhancement inside the InGaAs substrate on the distance between TCO nanoantennas and their diameter in Fig. 6. It is worthwhile noting, that the dielectric function of the doped InGaAs layer (doping $2 \times 10^{19} \text{ cm}^{-3}$) is calculated by

Fig. 4 Dependence of the 800-nm pump absorption enhancement inside the GaAs substrate on the distance between silver nanoantennas and their diameter



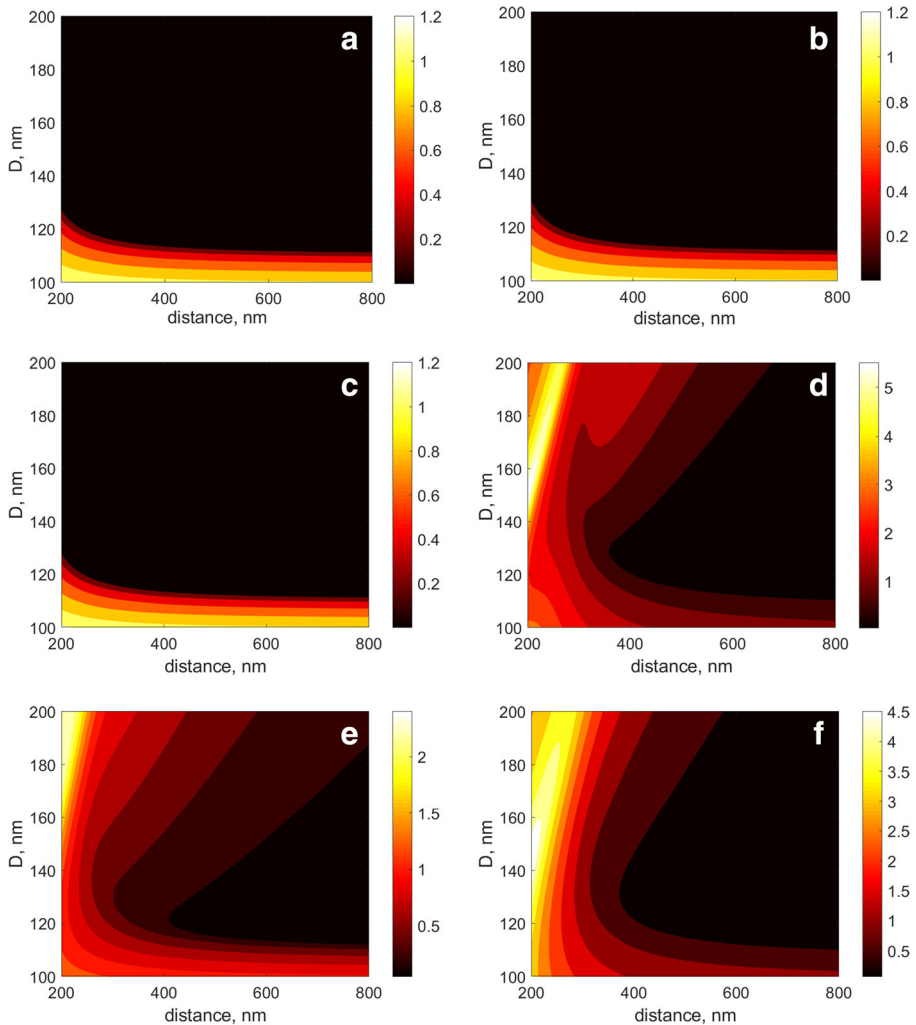


Fig. 5 Dependence of the 800-nm pump absorption enhancement inside the GaAs substrate on the distance between TCO nanoantennas and their diameter: (a)—AZO (ZnO:Al); (b)—GZO (ZnO:Ga); (c)—ITO (Sn-doped In_2O_3); (d)—TiN (deposited at 800 °C); (e)—TiN (deposited at 500 °C); (f)—ZrN

means of the Drude dielectric function $\epsilon_{\text{InGaAs}}(\omega) = 1 - \omega_p^2 / (\omega^2 + i\omega\gamma)$, where $\omega_p = 0.8\text{eV}$ and $\gamma = 0.014\text{eV}$ [41]. It is worthwhile noting, that GaAs substrate allows for a better enhancement (Fig. 5).

The absorption spectra of the nanocylinders were computed for each distance and are presented in Fig. 7 for both silver (a) and TiN (deposited at 800 °C) cases, making an assumption that nanowire diameter is 150 nm. The plot demonstrates that the absorption peak shifts towards lower frequencies as the distance increases for Ag case. For a given distance, the large peak in the spectrum matches the dipolar resonant plasmonic mode, and the smaller peaks at the higher frequencies are due to higher order modes. Comparison of the cases of two

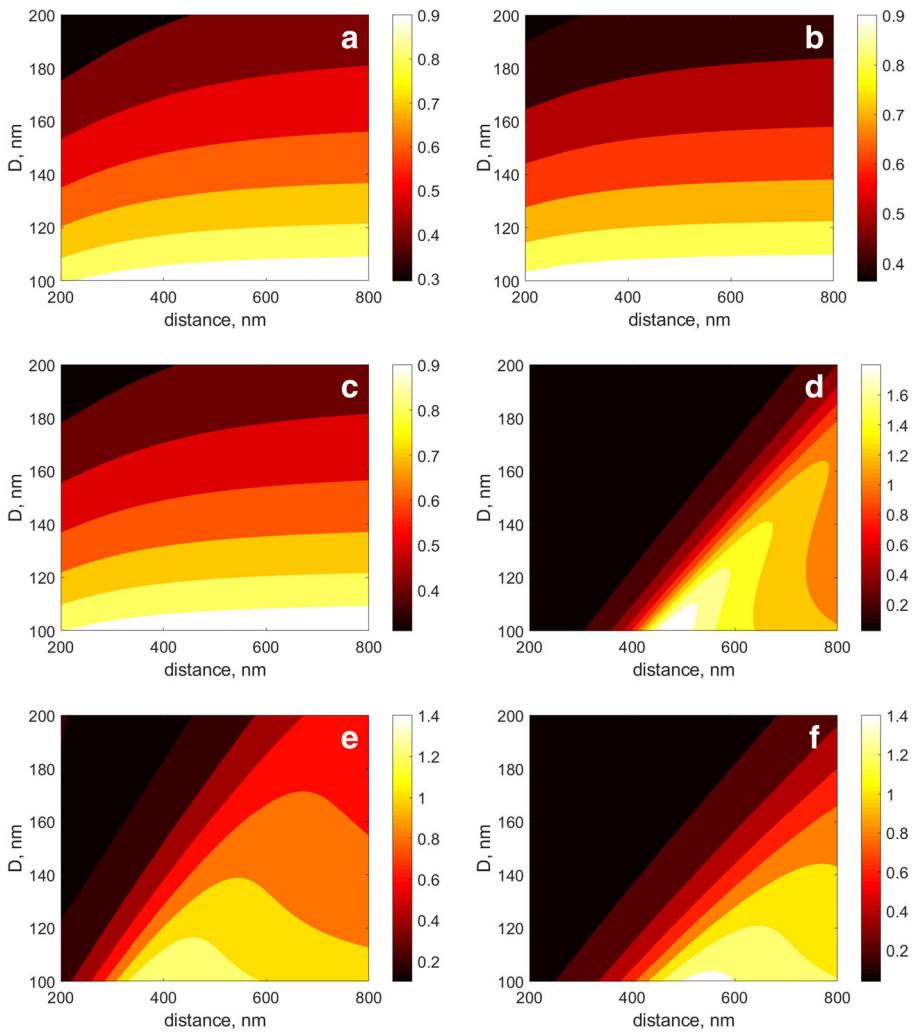


Fig. 6 Dependence of the 800-nm pump absorption enhancement inside the InGaAs substrate on the distance between TCO nanoantennas and their diameter: **(a)**—AZO (ZnO:Al); **(b)**—GZO (ZnO:Ga); **(c)**—ITO (Sn-doped In₂O₃); **(d)**—TiN (deposited at 800 °C); **(e)**—TiN (deposited at 500 °C); **(f)**—ZrN

materials for the same geometrical parameters leads to the conclusion that the resonance peak value has different positions. Whereas in silver embedded nanocylinders 150 nm in diameter, the peak gradually shifts to lower frequencies from 1800 THz (165 nm) towards 645 THz (465 nm) for nanocylinders spacing from 300 to 800 nm, correspondingly, embedded TiN nanocylinders of the same size demonstrate unchanged absorption peak position at 1070 THz (280 nm) with only absorption amplitude being dependent on nanowire spacing and moderately shifted broad stronger absorption peak between 315 THz (950 nm) and 103 THz (2910 nm) for nanowire spacing from 200 to 800 nm, correspondingly. Different behavior in silver and oxide nanocylinders can be associated with decoupling of the charge dipoles.

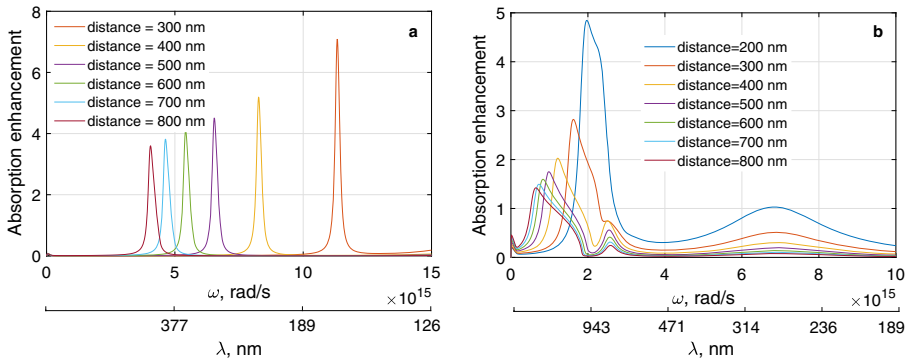


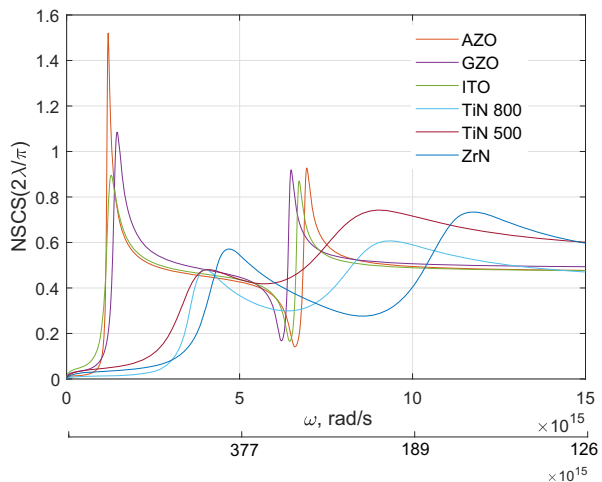
Fig. 7 Calculated absorption spectrum in case of GaAs substrate. For silver nanocylinders (a), for TiN (deposited at 800 °C) nanocylinders (b)

The calculated NSCS in case of the GaAs substrate is shown in Fig. 8 as a function of frequency and wavelength. The suppressed scattering is related to the cloaking phenomenon, where the scattering of all the modes is simultaneously and significantly reduced [42, 43]. All together, at the frequency of enhanced scattering, modes are at resonance.

5 Conclusion

To sum up, an approach to the PCA operation efficiency enhancement by optimized TCO plasmonic nanocylinders placed in its gap has been proposed. We believe that our results may be beneficial for many relevant applications, requiring compact and effective room-temperature terahertz sources, including spectroscopy, security imaging, and ultrafast data transmission. In other words, in this study, plasmonic properties of different TCO nanocylinders were computationally analyzed. Comparison between silver and TiN nanocylinders as absorption-enhancing plasmonic structures reveals fundamentally different

Fig. 8 Calculated NSCS in case of GaAs substrate



behavior of the resonant peak position dependence on nanowire spacing: In silver nanowire-enhanced substrates, resonant peak in absorption spectrum shifts towards the lower frequencies for the sparser nanowire spacing, whereas embedded TiN nanocylinders of the same size barely demonstrate change in absorption peak frequency, due to decoupling of the charge dipoles. The results presented here are important for plasmonic composites fabricated with electron beam lithography since we deal with the key fabrication parameters including distances between nanocylinders. Proper theoretical estimation of the optimal structure parameters is essential for further successful sample manufacturing. It is worthwhile noting that in case of TCO nanocylinders, absorption enhancement for NIR wavelengths, being relevant for present terahertz generation setup, reaches up to fivefold leading to 25-fold increase in terahertz radiation.

References

1. K. Kawase, Y. Ogawa, Y. Watanabe, H. Inoue, Non-destructive terahertz imaging of illicit drugs using spectral fingerprints, *Opt. Express* **11**, 2549–2554 (2003).
2. A. G. Davies, E. H. Linfield, M. B. Johnston, The development of terahertz sources and their applications, *Phys. Med. Biol.* **47**, 3679e–3689 (2002).
3. D. Banerjee, W. von Spiegel, M. D. Thomson, S. Schabel, H. G. Roskos, Diagnosing water content in paper by terahertz radiation, *Opt. Express* **16**, 9060–9066 (2008).
4. J. F. Federici, B. Schulkin, F. Huang, D. Gary, R. Barat, F. Oliveira, D. Zimdars, THz imaging and sensing for security applications—explosives, weapons and drugs, *Semicond. Sci. Technol.* **20**, S266–S280 (2005).
5. J. B. Jackson, M. Mourou, J. F. Whitaker, I. N. Duling, S. L. Williamson, M. Menu, G. A. Mourou, Terahertz imaging for non-destructive evaluation of mural paintings, *Opt. Commun.* **281**, 527–532 (2008).
6. Y. V. Grachev, X. Liu, S. E. Putilin, A. N. Tsyppkin, V. G. Bespalov, S. A. Kozlov, X.-C. Zhang, Wireless data transmission method using pulsed THz sliced spectral supercontinuum, *IEEE Photonics Technology Letters* **30**(1), 103–106 (2018).
7. M. Massaouti, C. Daskalaki, A. Gorodetsky, A. D. Koulouklidis, S. Tzortzakos, Detection of harmful residues in honey using terahertz time-domain spectroscopy, *Applied Spectroscopy*, **67**(11), 1264–1269 (2013).
8. P. U. Jepsen, R. H. Jacobsen, S. R. Keiding, Generation and detection of terahertz pulses from biased semiconductor antennas, *J. Opt. Soc. Am. B* **13**, 2424 (1996).
9. P. U. Jepsen, D. G. Cooke, M. Koch, Terahertz spectroscopy and imaging modern techniques and applications, *Laser Phot. Rev.* **5**, 124–166 (2011).
10. T. Gric, Surface-plasmon-polaritons at the interface of nanostructured metamaterials, *Progress In Electromagnetics Research M* **46**, 165–172 (2016).
11. T. Gric, M.S. Wartak, M. Cada, J.J. Wood, O. Hess & J. Pistora, Spoof plasmons in corrugated semiconductors, *Journal of Electromagnetic Waves and Applications* **29**(14), 1899–1907 (2015).
12. T. Gric, Spoof plasmons in corrugated transparent conducting oxides, *Journal of Electromagnetic Waves and Applications* **30**(6), 721–727 (2016).
13. J. B. Lassiter, J. Aizpurua, L. I. Hernandez, D. W. Brandl, I. Romero, S. Lal, J. H. Hafner, P. Nordlander, N. J. Halas, Close encounters between two nanoshells, *Nano Lett.* **8**, 1212–1218 (2008).
14. P. K. Jain, M. A. El-Sayed, Surface plasmon coupling and its universal size scaling in metal nanostructures of complex geometry: elongated particle pairs and nanosphere trimers, *J. Phys. Chem. C* **112**, 4954–4960 (2008).
15. H. Xu, J. Aizpurua, M. Ka'Il, P. Apell, Electromagnetic contributions to single-molecule sensitivity in surface-enhanced Raman scattering, *Phys. Rev. E* **62**, 4318–4324 (2000).
16. B. Kanté, A. de Lustrac, J. Lourtioz, In-plane coupling and field enhancement in infrared metamaterial surfaces, *Phys. Rev. B* **80**, 35108 (2009).
17. W. Q. Hu, E. J. Liang, P. Ding, G. W. Cai, Q. Z. Xue, Surface plasmon resonance and field enhancement in #-shaped gold wires metamaterial, *Opt. Express* **17**, 21843–21849 (2009).
18. V. M. Shalaev, Optical negative-index metamaterials, *Nat. Photonics* **1**, 41–48 (2007).
19. C. M. Soukoulis, S. Linden, M. Wegener, Negative refractive index at optical wavelengths, *Science* **315**, 47–49 (2007).

20. J. B. Pendry, A. Holden, D. J. Robbins, W. J. Stewart, Magnetism from conductors and enhanced nonlinear phenomena, *IEEE Trans. Microwave Theory Technol.* **47**, 2075–2084 (1999).
21. B. Lahiri, A. Z. Khokhar, R. M. De La Rue, S. G. McMeekin, N. P. Johnson, Asymmetric split ring resonators for optical sensing of organic materials, *Opt. Express* **17**, 1107–1115 (2009).
22. E.U. Rafailov, K. Fedorova, A. Gorodetsky, N. Bazieva, Recent progress in the development of quantum dot based devices in NIR and THz ranges SPIE Photonics West, San Francisco, 10111–97 (2017).
23. M. Unlu, M. R. Hashemi, C. W. Berry, S. Li, S. -H. Yang, M. Jarrahi, Switchable scattering meta-surfaces for broadband terahertz modulation, *Sci. Rep.* **4**, 5708 (2014).
24. C. W. Berry, N. Wang, M. R. Hashemi, M. Unlu, M. Jarrahi, Significant performance enhancement in photoconductive terahertz optoelectronics by incorporating plasmonic contact electrodes, *Nat. Commun.* **4**, 1622 (2013).
25. R. Leyman, A. Gorodetsky, N. Bazieva, G. Molis, A. Krotkus, E. Clarke and E. U. Rafailov, Quantum dot materials for terahertz generation and applications *Laser and Phot Review*, **8**, 1–8 (2016).
26. A. Al’u, N. Engheta, Wireless at the nanoscale: optical interconnects using matched nanoantennas, *Phys. Rev. Lett.* **104**, 213902 (2010).
27. D. Dietze, J. Darmo and K. Unterrainer, Guided Modes in Layered Semiconductor Terahertz Structures, *IEEE Journal of Quantum Electronics* **46**(5), 618–625 (2010).
28. G. V. Naik, V. M. Shalaev, A. Boltasseva, Alternative plasmonic materials: beyond gold and silver, *Adv. Mater.* **25**, 3264–3294 (2013).
29. A. Pokrovsky and A. Efros, Electrodynamics of metallic photonic crystals and the problem of left-handed materials, *Phys. Rev. Lett.* **89**, 093901 (2002).
30. G. Shvets, A. K. Sarychev, and V. M. Shalaev, Electromagnetic properties of three-dimensional wire arrays: photons, plasmons, and equivalent circuits, *Proc. SPIE* **5218**, 156 (2003).
31. P. Belov, R. Marques, S. Maslovski, I. Nefedov, M. Silveirinha, C. Simovski, and S. Tretyakov, Strong spatial dispersion in wire media in the very large wavelength limit, *Phys. Rev. B* **67**, 113103 (2003).
32. A. L. Pokrovsky and A. L. Efros, Nonlocal electrodynamics of two-dimensional wire mesh photonic crystals, *Physical Review B* **65**, 045110 (2002).
33. J. Elser, R. Wangberg, V. A. Podolskiy, Nanowire metamaterials with extreme optical anisotropy, *Appl. Phys. Lett.* **89**, 261102 (2006).
34. C. A. Balanis, *Advanced engineering electromagnetics* (Wiley, 1989).
35. Z. Ruan and S. Fan, Superscattering of light from subwavelength nanostructures, *Phys. Rev. Lett.* **105**, 013901 (2010).
36. S. Lepeshov, A. Gorodetsky, A. Krasnok, E. Rafailov, P. Belov, Enhancement of terahertz photoconductive antenna operation by optical nanoantennas, *Laser Photon. Rev.* **11**, 1600199 (2017)
37. A. Al’u, N. Engheta, Input impedance, nanocircuit loading, and radiation tuning of optical nanoantennas, *Phys. Rev. Lett.* **101**, 043901 (2008).
38. S. Lepeshov, A. Gorodetsky, A. Krasnok, N. Toropov, T. A. Vartanyan P. Belov, A. Alú, E. U. Rafailov, Boosting the Terahertz photoconductive antenna performance with optimized plasmonic nanostructures, *Scientific Reports* **8**, 6624 (2018).
39. I. El-Kady, M. M. Sigalas, R. Biswas, K. M. Ho, C. M. Soukoulis, Metallic photonic crystals at optical wavelengths, *Phys. Rev. B* **62**, 15299–15302 (2000).
40. C. W. Berry, M. Jarrahi, Principles of impedance matching in photoconductive antennas, *Journal of Infrared, Millimeter, and Terahertz Waves*, **33**(12), 1182–1189 (2012).
41. J. B. Khurgin, Replacing Noble Metals with Alternative Materials in Plasmonics and Metamaterials: how good an idea?, *Philos Trans A Math Phys Eng Sci.* **375**(2090), 20160068 (2017).
42. A. Alu, N. Engheta, Achieving transparency with plasmonic and metamaterial coatings, *Phys. Rev. E* **72**, 016623 (2005);
43. A. Alu and N. Engheta, Multifrequency optical invisibility cloak with layered plasmonic shells, *Phys. Rev. Lett.* **100**, 113901 (2008).